Square-lattice spiral magnet $Ba_2CuGe_2O_7$ in an in-plane magnetic field

A. Zheludev, S. Maslov, and G. Shirane
Physics Department, Brookhaven National Laboratory, Upton, New York 11973-5000

Y. Sasago, N. Koide, and K. Uchinokura
Department of Applied Physics, The University of Tokyo, 7-3-1 Hongo, Bunkyo-ku, Tokyo 113, Japan

D. A. Tennant and S. E. Nagler
Oak Ridge National Laboratory, Building 7692, MS 6393, P.O. Box 2008, Oak Ridge, Tennessee 37831
(Received 15 July 1997)

The magnetic structure of $Ba_2CuGe_2O_7$ is investigated by neutron diffraction in magnetic fields applied along several directions in the (a,b) plane of the crystal. In relatively weak fields, $H \lesssim 0.5$ T, the propagation vector of the spin spiral rotates to form a finite angle with the field direction. This angle depends on the orientation of **H** itself. The rotation of the propagation vector is accompanied by a reorientation of the plane of spin rotation in the spiral. The observed behavior is well described by a continuous-limit form of a free-energy functional that includes exchange and Dzyaloshinskii-Moriya interactions, as well as the Zeeman energy and an empirical anisotropy term. [S0163-1829(97)00245-2]

I. INTRODUCTION

Incommensurate magnetic structures in insulators are as a rule caused by a competition between two or more magnetic interactions. In the classic description of a spiral spin structure in MnO_2 Yoshimori attributed the spiral spin arrangement to a competition between two distinct antiferromagnetic (AF) Heisenberg exchange interactions in the crystal.[1] We shall refer to this kind of spiral state as ''exchange spiral.'' An alternative mechanism is realized in a few systems with noncentric crystal structures. Isotropic exchange terms in the Hamiltonian compete with Dzyaloshinskii-Moriya (DM) interactions.[2,3] The former are proportional to $(\mathbf{S}_1 \cdot \mathbf{S}_2)$, i.e., the scalar product of interacting spins, and thus favor a collinear state. The DM term is given by a *vector* product and is usually written as $(\mathbf{D} \cdot [\mathbf{S}_1 \times \mathbf{S}_2])$, where **D** is the so-called Dzyaloshinskii vector that characterizes the oriented bond between spins $\mathbf{S}_1$ and $\mathbf{S}_2$. DM interactions favor a relative angle of 90° between spins. Unlike isotropic exchange, DM coupling is of relativistic origin, i.e., is a result of spin-orbit interactions, and ties the spin system to the underlying crystal lattice via orbital degrees of freedom. The best known examples of real compounds where this second scenario (''relativistic spiral'') is realized are the MnSi (Refs. 4–7) and FeGe.[8,9] Recently we have observed an incommensurate spiral spin structure in $Ba_2CuGe_2O_7$ and explained it within this framework.[10–12]

While the ground states in both models (''exchange'' and ''relativistic'') may be similar, under certain conditions they behave very differently in applied magnetic fields. If only isotropic exchange interactions are present, the direction of magnetic field is irrelevant to the spin structure: the spin space may be freely rotated without a change in interaction energy and the spins are not tied to any particular direction in the crystal. For ''relativistic'' spiral magnets the spin structure in an external field **H** in general may be strongly dependent on the relative orientation of **H** and the Dzyaloshinskii vectors, although in several special cases of high-symmetry crystal structures this is not so. In FeGe, for example, the interactions of each spin with its neighbors are characterized by Dzyaloshinskii vectors pointing in all three equivalent orthogonal directions. In this situation applying a very small magnetic field always leads to a reorientation of the spin rotation plane normal to the field direction, and, consequently, the propagation vector becomes aligned along the field. The length of the magnetic propagation vector is to a good approximation field independent.

In materials of lower crystal symmetry, as, for example, in hexagonal $CsCuCl_3$ (Refs. 13–16) and $RbMnBr_3$,[17,18] or tetragonal $Ba_2CuGe_2O_7$, the spin rotation plane cannot be freely re-oriented without affecting the Dzyaloshinskii energy. As a result, the magnetic structure undergoes drastic changes for certain field geometries, and the length of the propagation vector becomes strongly field dependent. An extreme example of this behavior is the commensurate-incommensurate transition that we have recently observed and theoretically analyzed for $Ba_2CuGe_2O_7$.[11,12] As a magnetic field is applied along the unique c axis of the tetragonal structure, the initially uniform sinusoidal spin spiral is distorted. In a non-zero field it may be viewed as a soliton lattice, a regular arrangement of antiphase domain wall boundaries separating regions of commensurate antiferromagnetic spin-flop phase. As the field is increased, the period of the structure, given by the distance between solitons, increases and diverges at some critical field, $H_c \approx 2.1$ T, above which a commensurate spin-flop state is observed.

In this work we address the field dependence of the magnetic structure of $Ba_2CuGe_2O_7$ in a magnetic field **H** applied in the (a,b)-tetragonal plane. We show that the square-lattice spin arrangement in this geometry allows an almost unhindered reorientation of the spin plane with only a very small change in the period of the structure, much like in cubic FeGe. The principal difference between FeGe and $Ba_2CuGe_2O_7$ is that in the former material the propagation

 © 1997 The American Physical Society

vector rotates towards the direction of applied field. We find that for $Ba_2CuGe_2O_7$ the propagation vector tends to form a finite angle with **H**, that depends on the orientation of **H** itself. The rotation of the propagation vector with increasing field is continuous. The observed behavior is found to be in very good agreement with theoretical predictions based on a two-dimensional generalization of the simple Ginzburg-Landau energy functional that we have previously employed to describe the Dzyaloshinskii transition in $Ba_2CuGe_2O_7$.

II. EXPERIMENTAL PROCEDURES

A single crystal of $Ba_2CuGe_2O_7$, the same sample that was used in our previous work, was studied in a neutron diffraction experiment at the High Flux Isotope Reactor at Oak Ridge National Laboratory, on the HB-3 triple-axis spectrometer. The sample, roughly $4\times4\times4$ mm^3 in volume, was mounted in a small aluminum container where it was secured with compressed Al foil. The container was in turn mounted on a precision microgoniometer, that was used to align the (a,b) crystallographic plane in the scattering plane of the spectrometer, prior to setting up the sample in the cryomagnet.

The magnetic field was produced by using a split-coil *horizontal-field* superconducting solenoid. The construction of the magnet provides two pairs of windows for the incident and outgoing neutron beams. The larger pair of windows, each window being $\pm30°$ wide, is oriented perpendicular to the field direction. An additional narrower pair of windows ($\pm15°$) is positioned around the direction of magnetic field. Within the cryomagnet the sample could be manually rotated around the vertical axis *in situ*. We estimate the uncertainty in the initial alignment of the sample relative to the field direction to be of the order of 1°. After this initial setting the relative rotation of the sample in the magnet was done with much higher accuracy, $\approx0.1°$, as it could be directly followed by monitoring the in-plane Bragg reflections. Measurements were done for several values of the angle ψ between the magnetic field and the $[110]$ direction, namely, for $\psi=45.0°$, 50.0°, 52.9°, 57.5°, 60.2°, 61.7°, 61.9°, 71.5°, and 75.2°, the field always being applied in the (a,b) plane of the crystal. Although the magnet is capable of much higher field strengths, stray fields are a serious problem, and all the measurements were done in $H\leqslant2$ T. The temperature of the sample was controlled by a standard He-flow cryostat, allowing us to perform measurements in the temperature range 1.8–10 K. As we will discuss in detail below, the magnetic structure changes in applied fields, but this effect shows a very strong field hysteresis. To avoid this complication all the measurements were done using field cooling. The sample was first warmed up to $T=6$ K, well above the temperature of magnetic ordering $T_N=3.2$ K,[10] the desired strength and direction of the magnetic field were set, and only then was the sample brought down to base temperature, $T=1.8$ K, where most of the measurements were performed.

At all times the measurements were done in three-axis mode to reduce the signal to background ratio. $60'-40'-40'-120'$ collimations were used with pyrolitic graphite (PG) (002) reflections for monochromator and analyzer, with 14.7 meV neutron energy and a PG filter positioned in front of the sample.

III. EXPERIMENTAL RESULTS

The crystal and magnetic structures of $Ba_2CuGe_2O_7$ are discussed in detail in our previous publications on the subject,[10–12] and only the most essential features are reviewed here. The magnetic Cu^{2+} ions form a square lattice in the (a,b) tetragonal plane of the crystal. The principal axes of this square lattice, hereafter referred to as the x and y axis, are along the $[110]$ and $[1\bar{1}0]$ directions, respectively. To complete the coordinate system we shall choose the z axis to run along $[001]$. In the ordered phase (below $T_N=3.2$ K) the spins lie in the $(1,-1,0)$ plane and the magnetic propagation vector is $(1+\zeta,\zeta,0)$, where $\zeta=0.027$. The magnetic structure is a distortion of a Néel spin arrangement: a translation along $(\frac{1}{2},\frac{1}{2},0)$ induces a spin rotation by an angle $\alpha=\pi/\zeta\approx8.6°$ (relative to an exact antiparallel alignment) in the $(1,-1,0)$ plane. Along the $[1\bar{1}0]$ direction nearest-neighbor spins are perfectly antiparallel. Nearest-neighbor spins from adjacent Cu planes are aligned parallel to each other.

Obviously, domains with propagation vectors $(1+\zeta,\pm\zeta,0)$ are equivalent and always equally represented in a zero-field-cooled sample. This can be seen in Fig. 1(a) which shows a contour plot of elastic intensities measured at $T=1.8$ K on a mesh of points around the $(1,0,0)$ position in zero field. We clearly see four magnetic reflections symmetrically grouped around the AF zone center. The two pairs of peaks, $(1\pm\zeta,\pm\zeta,0)$ and $(1\pm\zeta,\mp\zeta,0)$, correspond to the two magnetic domains. The propagation vector **q**, measured relative to the AF zone center, is strictly along the $[110]$ (or $[1\bar{1}0]$) direction. The weak feature around $(1,0,0)$ is an artifact that is temperature independent and was previously identified as a multiple scattering peak.[10] Cooling the sample in a very weak magnetic field (≈10 mT) always produces a single-domain structure.

When a magnetic field is applied along the $[100]$ direction the diffraction pattern begins to change. The propagation vector **q** starts to rotate in reciprocal space towards the direction of applied field [Fig. 1(b)], eventually becoming perfectly aligned with it [Fig. 1(c)]. Note that all this happens in rather small fields, less than 0.3 T. This is to be compared with the field along the c axis, $H_c\approx2.1$ T, that is required to induce the CI transition studied previously. Since $H_c\mu_B\approx|\mathbf{D}|$, we can conclude that for a horizontally applied field the rotation of **q** occurs in fields that are an order of magnitude smaller than the Dzyaloshinskii energy.

In the following discussion it is convenient to introduce notations for some angles in our experiment (Fig. 2). We shall denote by ψ the angle between the magnetic field **H** and the $[110]$ direction in the crystal. ϕ will stand for the angle between $[110]$ and **q**. Using $[110]$ as a reference is very convenient since i) $\phi=0$ for $H=0$ and ii) the principal axes of the square-lattice arrangement of the magnetic Cu sites in $Ba_2CuGe_2O_7$ are along $[110]$ and $[1\bar{1}0]$, respectively. In these terms, for $\psi=\pi/4$, as H is increased, ϕ continuously increases from 0 to $\pi/4$.

For several directions of the magnetic field we have performed careful measurements of $\phi(H)$. The results are summarized in Fig. 3. Measurements with $\psi<61°$ were done on the magnetic satellites around the $(1,0,0)$ AF zone center,

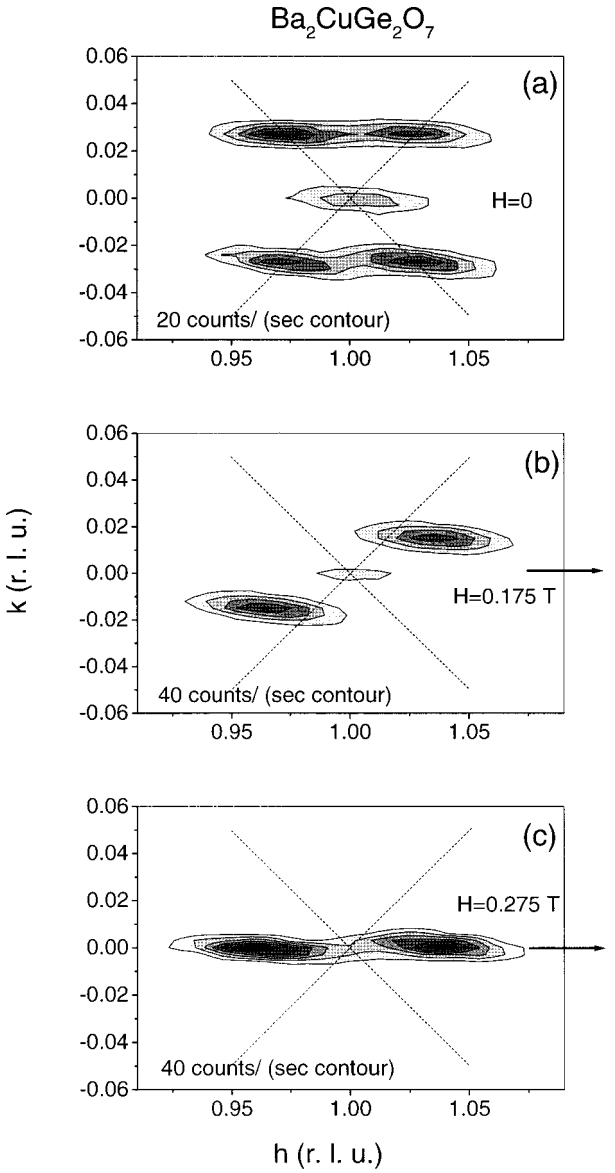

FIG. 1. Contour plots of elastic neutron scattering intensity measured in $Ba_2CuGe_2O_7$ around the $(1,0,0)$ antiferromagnetic zone-center for three values of magnetic field applied along the $[100]$ direction. Plot (a) was measured for a zero-field-cooled sample, and field cooling was used for plots (b) and (c).

and those around $(2,1,0)$ were used for higher values of ψ. This was necessary to work around the geometrical constraints set by the cryostat windows. As mentioned, for $\psi=\pi/4$ the propagation vector starts out at $\phi=0$ for $H=0$ and rotates all the way towards the field direction ($\phi=\psi=\pi/4$), as in the case of FeGe. For arbitrary field direction though, while ϕ levels off above $H\approx 0.5$ T, it does so at a smaller value, i.e., before **q** reaches the direction of applied field. If we plot ϕ measured at a relatively high field, $H=2$ T, we find that the saturation value for ϕ is always $\pi/2-\psi$ (Fig. 4). Thus at high fields the $(1,0,0)$ vector always bisects the angle formed by the magnetic field **H** and the propagation vector **q**. Note that in all cases we have $\psi\geqslant\pi/4$. If the magnetic field forms a smaller angle with the $[110]$ direction, the magnetic domain with propagation vector $(1+\zeta_h,\zeta_k,0)$, $\zeta_h\zeta_k>0$ is destroyed, and the diffraction

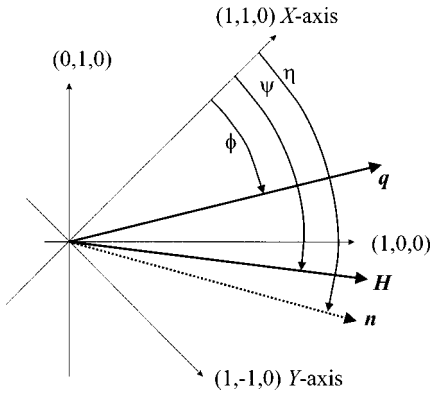

FIG. 2. Experimental geometry: The magnetic field **H** is applied in the (a,b) crystallographic plane at an angle ψ to the $[110]$ direction. The propagation vector **q** and the normal to the plane of spin rotations form angles ϕ and η with the $[110]$ direction, respectively.

intensity completely shifts over into the $\zeta_h\zeta_k<0$ domain, returning us to the situation when ψ is effectively greater than $\pi/4$. This fact has been verified experimentally.

An important experimental result is that for all directions and of the applied magnetic field the length of the magnetic propagation vector $|\mathbf{q}|$ is only weakly field dependent. This can be seen in Fig. 5 that shows the trajectory traced by the propagation vector in reciprocal space as the magnetic field is increased. For $\psi=\pi/4$ this trajectory is an almost perfect circular arc that starts out at $\phi=0$ and continues all the way to $\phi=\pi/4$ [Fig. 5(a)]. For arbitrary ψ we see that $|q|$ is indeed slightly field-dependent and the trajectory has a characteristic *S* shape. This, however, is a weak effect, barely detectable with the precision of our experiment, limited by the *Q* resolution of the spectrometer.

Having discussed the field dependence of the propagation vector, we now turn to that of the spin orientation. Typically to solve the magnetic structure one has to measure the intensities of several Bragg peaks. In the present experiment, however, we did not have this luxury. The severe geometri-

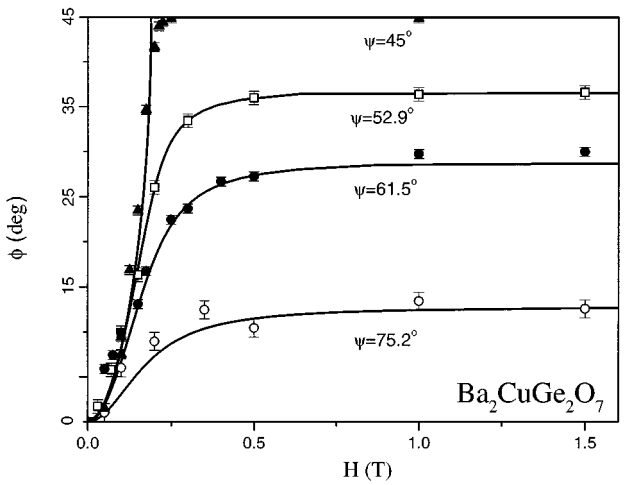

FIG. 3. Field dependence of the direction of magnetic propagation vector measured in $Ba_2CuGe_2O_7$ for several directions of magnetic field applied in the (a,b) crystallographic plane. The solid lines represent a theoretical fit to the data, described in the text.

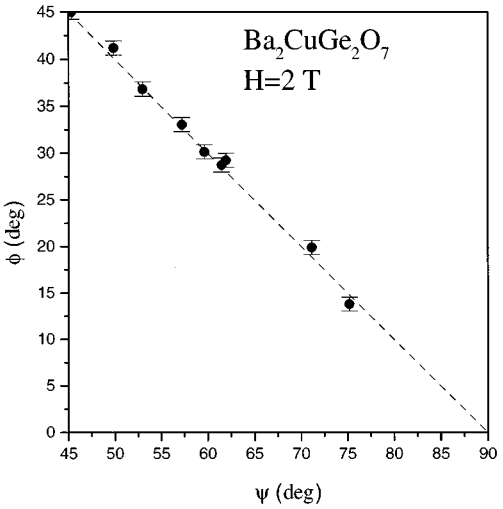

FIG. 4. ϕ, the direction of magnetic propagation vector, measured in $Ba_2CuGe_2O_7$ as a function of ψ, the direction of the external magnetic field for $H=2$ T. The dashed line shows the theoretical result.

cal constraints imposed by the narrow cryostat windows eliminate simultaneous access to several magnetic peaks. Many of these could be observed by rotating the sample within the magnet, however, in this case the direction of the magnetic field relative to the sample is changed. Only in the case of $\psi=\pi/4$, thanks to the presence of two orthogonal pairs of windows, could we simultaneously observe more than one set of magnetic satellites, namely those around (1,0,0) and (0,1,0). The intensities of these reflections are plotted against H in Fig. 6 for $\psi=\pi/4$. These data are not sufficient to independently determine the magnetic structure for each value of applied field. We can however assume that for all cases, just as for $H=0$, the spin arrangement is a flat magnetic spiral, with the normal to the spin rotation plane confined in the (a,b) plane of the crystal. The assumption is quite reasonable if we consider that in our experiments $H\leqslant 2$ T and $\mu_B H\lesssim 0.1$ meV, so the Zeeman energy is at least an order of magnitude smaller than the exchange energy ($4JS\approx 1$ meV). A slight conical distortion of the planar spiral structure is of course inevitable in finite magnetic fields, but the tilt towards the direction of **H** will remain very small. If we denote by η the angle between $[110]$ and $\hat{\mathbf{n}}$, the normal to the spin rotation plane ($\eta=\pi/2$ for $H=0$), the intensities of magnetic satellites around (1,0,0) and (0,1,0) are determined by the spin polarization factors in the neutron diffraction cross section:

$$I_{(100)}\propto 1+\cos^2(\eta-\pi/4),$$

$$I_{(010)}\propto 1+\sin^2(\eta-\pi/4). \qquad (1)$$

From Fig. 6 we see that at high fields $I_{(100)}$ increases by roughly a third of its original value, while $I_{(010)}$ decreases by roughly the same amount. This observation is consistent with $\eta=\pi/4$ at high fields, as could be expected: a sufficiently strong magnetic field will always align the spin rotation plane perpendicular to itself, independent of the field direction. For arbitrary ψ we therefore expect $\eta=\psi$ in sufficiently high fields. Experimentally, for all directions of magnetic

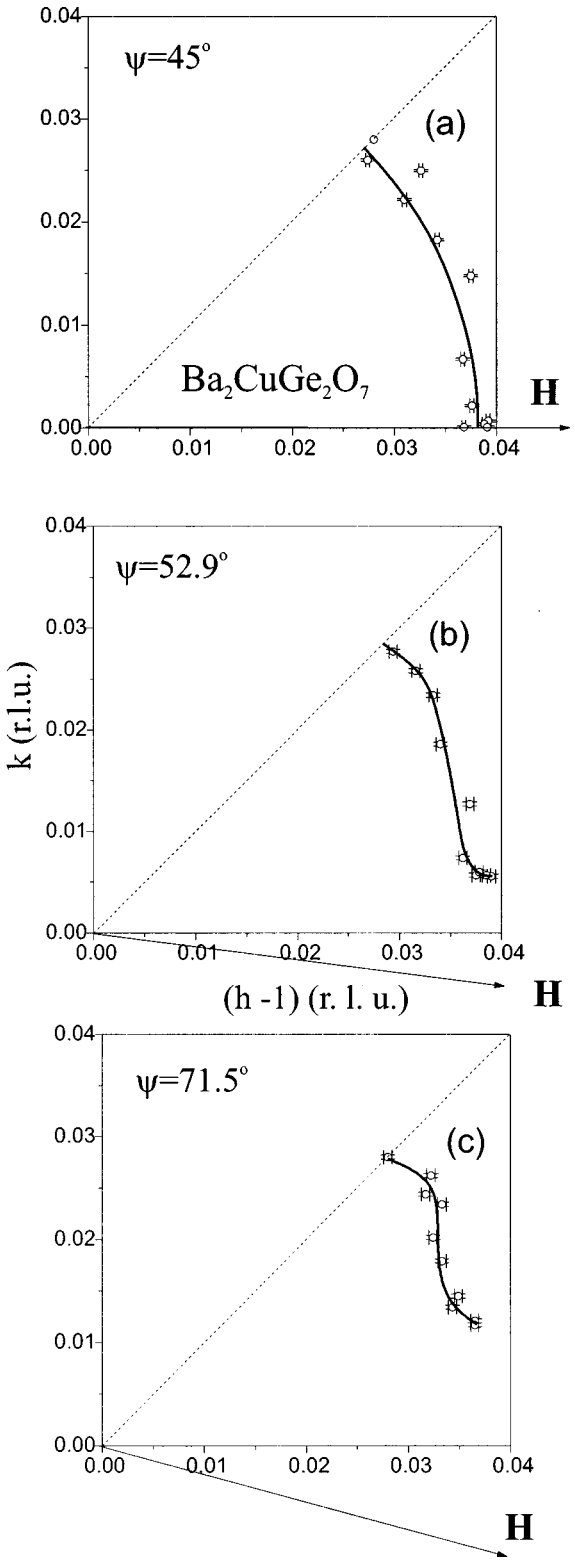

FIG. 5. Measured trajectories traced by the magnetic propagation vector in $Ba_2CuGe_2O_7$ as a magnetic field is applied in the (a,b) plane of the crystal. The solid lines are guides for the eye.

field studied, this rule was found to be consistent with the observed intensity increase in the satellites around (1,0,0) or (2,1,0) that occurs upon increasing the magnetic field from $H=0$ to $H=2$ T.

As will be discussed in detail in the next section, theory predicts that for *arbitrary* values of H one has

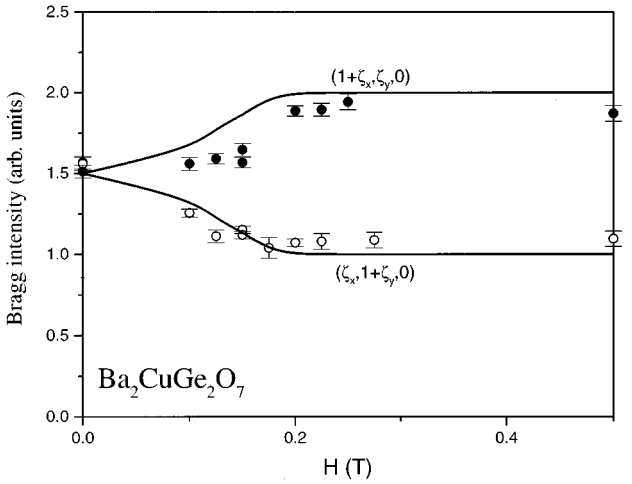

FIG. 6. Measured intensities of magnetic satellites around the (1,0,0) and (0,1,0) antiferromagnetic zone centers in $Ba_2CuGe_2O_7$ plotted as a function of magnetic field applied along the a axis. The solid lines are the theoretically predicted dependences, as described in the text.

$$\phi = \pi/2 - \eta. \tag{2}$$

Since $\phi(H)$ is directly measured in our experiments, we can plot the expected field dependencies of $I_{(100)}$ and $I_{(010)}$ using Eqs. (1) and (2). These are shown in solid lines in Fig. 6 and are reasonably consistent with experimental data.

We can now summarize all the experimental results in a short list of ''rules:'' (i) As the magnetic field is increased, **q** rotates in reciprocal space for small H, but slows down and eventually stops for $H \gtrsim 0.5$ T; (ii) $|\mathbf{q}|$ is only weakly field dependent; (iii) at high fields the $[100]$ direction bisects the angle formed by the vectors **H** and **q**; (iv) at high fields $\hat{\mathbf{n}}$ is pointing along the direction of applied field; and (v) it appears that for arbitrary H the $[100]$ direction always bisects the angle formed by the vectors **q** and $\hat{\mathbf{n}}$.

IV. THEORY

We shall now demonstrate that the observed behavior can be well understood using a generalization of the approach that we have previously employed to quantitatively analyze the Dzyaloshinskii transition in $Ba_2CuGe_2O_7$. While in our previous studies the direction of the propagation vector remained constant, which enabled us to use an effectively one-dimensional model, in the present experiment **q** rotates in the (a,b) plane, and we have to extend our expression for the free energy of the spin structure to work in two dimensions.

A. The continuous limit

In general, any almost-antiferromagnetic spin structure can be described in terms of the unit vector $\hat{\mathbf{m}}(\mathbf{r})$ of local staggered magnetization. This is the continuous limit, when nearest-neighbor spins are almost antiparallel and, in consequence, the magnetic propagation vector is close to that of a Néel structure. For a ''relativistic'' spiral, such as the one in $Ba_2CuGe_2O_7$, the continuous approximation is expected to work well when $|\mathbf{D}|$, $\mu_B H \ll J$, a condition well satisfied in our experiments.

The simplest form of the free energy that for $H=0$ gives a planar spin spiral with propagation vector along x and the spins rotating in the (x,z) plane, is $F = \rho_s/2 \int dxdy (\partial_x \hat{\mathbf{m}} - \alpha/\Lambda \ \mathbf{e}_y \times \hat{\mathbf{m}})^2$, where $\rho_s \simeq JS^2$ is the temperature dependent spin stiffness (see Refs. 11 and 12), $\Lambda = a/\sqrt{2}$ (a being the lattice constant) is the nearest neighbor Cu-Cu distance, and α is the angle by which spins are rotated at one step of the spiral. For the ''relativistic'' spiral in $Ba_2CuGe_2O_7$, $\alpha = -\arctan|\mathbf{D}|/J \approx 10°$. Of course, on a square lattice the spiral can equally well propagate in the direction of the symmetrically equivalent y axis [with spins rotating in the (y,z) plane], and a similar term where y is interchanged with x has to be added to the free energy functional. The purely ferromagnetic interactions between the Cu layers in $Ba_2CuGe_2O_7$ (Ref. 10) can be accounted for by including the term $\rho_s \gamma/2 \int dxdy \ \ (\partial_z \hat{\mathbf{m}})^2$, where γ is the spin stiffness anisotropy factor, $\gamma \approx 0.03$ for $Ba_2CuGe_2O_7$. Finally, the interaction with external magnetic field is given by the Zeeman term $E_Z = -\int dxdy \ [(\chi_\perp - \chi_\parallel)(\mathbf{H} \times \hat{\mathbf{m}})^2/2 + \chi_\parallel H^2/2]$ (for details see Refs. 11 and 12). In this last expression $\chi_{||}$ and $\chi_\perp$ are the longitudinal and transverse local staggered susceptibilities of the almost AF spin structure, respectively. For the classical spin model at $T=0$ one gets $\chi_\perp = (g\mu_B)^2/(8J\Lambda^2)$ and $\chi_\parallel = 0$. Combining all of the above terms gives us the simplest expression for the free energy per Cu plane, that is consistent with symmetric properties of the system and gives the ''right answer'' for $H=0$:

$$F = \int dxdy \left\{ \frac{\rho_s}{2} \left[\left(\partial_x \hat{\mathbf{m}} - \frac{\alpha}{\Lambda} \mathbf{e}_y \times \hat{\mathbf{m}} \right)^2 + \left(\partial_y \hat{\mathbf{m}} - \frac{\alpha}{\Lambda} \mathbf{e}_x \times \hat{\mathbf{m}} \right)^2 + \gamma (\partial_z \hat{\mathbf{m}})^2 \right] - \frac{(\chi_\perp - \chi_\parallel)(\mathbf{H} \times \hat{\mathbf{m}})^2}{2} - \frac{\chi_{||} H^2}{2} \right\}. \tag{3}$$

B. Zero magnetic field

Let us first consider the system in the absence of a magnetic field. We want to find a solution for a *general* direction of the propagation vector in the (x,y) plane. For the case when **q** forms the angle ϕ with the x axis it is convenient to change the coordinate system to (x',y',z') with x' along the propagation vector, y' perpendicular to x' in (x,y) plane, and $z'=z$. The derivatives and unit vectors are changed according to

$$\partial_x = \cos\phi \partial_{x'} - \sin\phi \partial_{y'}, \tag{4}$$

$$\partial_y = \cos\phi \partial_{y'} + \sin\phi \partial_{x'},$$

$$\mathbf{e}_x = \cos\phi \mathbf{e}_{x'} - \sin\phi \mathbf{e}_{y'}, \tag{5}$$

$$\mathbf{e}_y = \cos\phi \mathbf{e}_{y'} + \sin\phi \mathbf{e}_{x'}.$$

With these expressions Eq. (3) after some algebra can be rewritten as

$$F=\int dxdy\left[\frac{\rho_s}{2}\left((\partial_{x'}\hat{\mathbf{m}})^2+(\partial_{y'}\hat{\mathbf{m}})^2+\gamma(\partial_{z'}\hat{\mathbf{m}})^2-\frac{2\alpha}{\Lambda}(\cos 2\phi\,\mathbf{e}_{y'}+\sin 2\phi\,\mathbf{e}_{x'})\cdot\partial_{x'}\hat{\mathbf{m}}\times\hat{\mathbf{m}}\right.\right.$$
$$\left.\left.-\frac{2\alpha}{\Lambda}(\cos 2\phi\,\mathbf{e}_{x'}+\sin 2\phi\,\mathbf{e}_{y'})\cdot\partial_{y'}\hat{\mathbf{m}}\times\hat{\mathbf{m}}+\frac{\alpha^2}{\Lambda^2}(1+l_{z'}^2)\right)-(\chi_\perp-\chi_\parallel)(\mathbf{H}\times\hat{\mathbf{m}})^2/2-\chi_\parallel H^2/2\right]. \quad (6)$$

For $H=0$, since we have selected x' to be the direction of the propagation vector, $\partial_{x'}\hat{\mathbf{m}}\neq 0$, while $\partial_{y'}\hat{\mathbf{m}}=\partial_{z'}\hat{\mathbf{m}}\equiv 0$. It is straightforward to verify that the above expression is minimized when (i) $\hat{\mathbf{m}}(\mathbf{r})$ is periodic with the period $2\pi/\alpha$ and (ii) along its vector of propagation $\hat{\mathbf{m}}$ uniformly rotates in a plane that is perpendicular to $\cos 2\phi\,\mathbf{e}_{y'}+\sin 2\phi\,\mathbf{e}_{x'}=\cos\phi\,\mathbf{e}_y+\sin\phi\,\mathbf{e}_x$, i.e., the ''bisection rule'' $\eta=\pi/2-\phi$ formulated in the previous section is satisfied. In zero external field all spiral structures that conform with this bisection rule are degenerate, i.e., they have the *same* free energy.

C. Nonzero in-plane field

It is now easy to understand what happens in the case $H>0$. From all the possible spiral structures, energetically degenerate at $H=0$, the system will pick the one that takes the most advantage of the Zeeman energy $-(\mathbf{H}\times\hat{\mathbf{m}})^2$, namely that which has its spin plane normal to the field direction. Independent of the value of H (always assuming $\mu_B H\ll J$), instead of two equivalent domains seen at $H=0$ one gets a single domain with $\phi=\pi/2-\psi$ and $\eta=\psi$. The particular case of $\mathbf{H}\|(\mathbf{e}_x+\mathbf{e}_y)$ is of special interest. In this case the propagation vector is also directed along $(\mathbf{e}_x+\mathbf{e}_y)$ and one has a ''screw-type'' spiral with all spins perpendicular to the propagation axis. Such a ''screw-type'' structure is realized in MnSi and FeGe for arbitrary direction of $\mathbf{q}$.

While the above result accounts for the experimentally observed behavior for $H\gtrsim 0.5$ T, we still have to explain why the rotations of the spin plane and the propagation vector are continuous and in small fields some intermediate structure is realized. Obviously this is due to some anisotropy effects that pick the propagation vector along $[1\bar{1}0]$ (or $[\bar{1}\bar{1}0]$) and the normal to the spin plane along $[1\bar{1}0]$ (or $[110]$) for $H=0$ in the first place. The most likely source of anisotropy is spin-orbital interaction. For the present discussion however, the actual origin of magnetic anisotropy is of little importance: we can take it into account by introducing a phenomenological term into Eq. (3). This is done under the assumption that the anisotropy energy E_A, as well as the Zeeman energy E_Z, are much smaller than the energy scales of Dzyaloshinskii or exchange interactions. Neither magnetic field, nor anisotropy can distort any of the planar spiral structures in this limit. Their only effect is to pick the one that gives the greatest gain in Zeeman and anisotropy energies. E_A can now be written as a function of η or ϕ, which is in essence the same thing, since for all the structures we are dealing with $\eta\equiv\pi/2-\phi$. Since at $H=0$ we know from experiment that $\eta=\pi/2$,[10] the anisotropy term must be a minimum at this point. It must also comply with the fourfold symmetry of the crystal, i.e., it must be invariant under $\eta\rightarrow\eta+\pi/2$. In the most general case it is written as $E_A=-A_1\cos(4\eta)-A_2\cos(8\eta)\ldots$. It is also convenient to rewrite the Zeeman energy in terms of ϕ and ψ: $E_Z=-(\chi_\perp-\chi_\parallel)(\mathbf{H}\times\hat{\mathbf{m}})^2/2=-(\chi_\perp-\chi_\parallel)H^2\cos^2(\eta-\psi)/2$. Minimizing E_Z+E_A with respect to η we obtain

$$H^2=-\frac{8A_1\sin 4\eta+16A_2\sin 8\eta+\cdots}{(\chi_\perp-\chi_\parallel)\sin 2(\eta-\psi)}, \quad (7)$$

or, substituting $\eta=\pi/2-\phi$,

$$H^2=\frac{8A_1\sin 4\phi+16A_2\sin 8\phi+\cdots}{(\chi_\perp-\chi_\parallel)\sin 2(\phi+\psi)}. \quad (8)$$

This expression gives us the direction of the propagation vector and the orientation of the spin rotation plane for arbitrary H.

D. Comparison with experiment

We can now verify that the analytical results obtained in the previous section are consistent with our experiments on $Ba_2CuGe_2O_7$. To begin with, all the approximations that were made in the above calculations are justified. Indeed, the anisotropy energy in $Ba_2CuGe_2O_7$ corresponds to magnetic fields of several tenths of a T, fields in which the propagation vector actively rotates. The energy of Dzyaloshinskii interactions, as previously mentioned, corresponds to fields of the order of 2 T, while the exchange energy is roughly 10 times as large.

Equation (8) can be directly used to fit the experimentally measured $\phi(H)$. The solid lines in Fig. 3 are the result of a *global* fit of this expression to all our data collected at different ψ. The only adjustable parameter was the anisotropy coefficient $\tilde{A}_1\equiv A_1/(\chi_\perp-\chi_\parallel)$, while we assumed $A_2=A_3=\cdots=0$. The refined value for $\tilde{A}_1$ is $1.95(0.13)\times 10^{-3}$ T^2. The accuracy of the single-parameter fit is quite remarkable.

It is interesting to note that our theory predicts qualitatively different behaviors for the cases of $\psi=\pi/4$ and $\psi>\pi/4$, which is particularly easy to understand in the case $A_2=A_3=\cdots=0$. For $\psi=\pi/4$, Eq. (8) turns into $H^2=8A_1\sin 4\phi/(\chi_\perp-\chi_\parallel)\sin 2\eta=16A_1\sin 2\phi/(\chi_\perp-\chi_\parallel)$. We see that $\phi(H)$ changes continuously for $H^2\leqslant 16A_1/(\chi_\perp-\chi_\parallel)$, has a kink at this value and remains constant (equal to $\pi/4$) above this threshold. On the other hand, for $\psi>\pi/4$ the ϕ approaches $\pi/2-\psi$ asymptotically in high fields, $\phi(H)$ is a smooth function and there is no threshold field. Precisely this kind of behavior is observed in experiment (Fig. 3).

The limited data that we have for the orientation of the spin plane are also totally consistent with theory. The only effect that our theoretical model fails to account for is the observed slight variation of $|\mathbf{q}|$. This phenomenon may be a result of corrections to the continuous-limit approximation

that we have ignored. Alternatively, it may be a purely quantum effect, related to the small value ($S=1/2$) of spins involved and the quasi-two-dimensional nature of the system.

V. CONCLUDING REMARKS

Again we emphasize the key difference between FeGe and MnSi on one side, and $Ba_2CuGe_2O_7$ on the other. In the former two systems the Dzyaloshinskii vector is pointing along the bond between interacting spins, while in $Ba_2CuGe_2O_7$ **D** is orthogonal to this bond. As a result, in FeGe the normal to the spin plane $\hat{\mathbf{n}}$, and the propagation vector **q** are always collinear. In contrast, in $Ba_2CuGe_2O_7$ this colinearity is replaced by the ''bisection rule:'' **q** and $\hat{\mathbf{n}}$ form equal angles with the *a* axis of the crystal, but are not colinear.

In conclusion, we believe that the present work gives a fairly complete picture of the rather exotic *static* magnetic properties of the square-lattice Dzyaloshinskii-Moriya antiferromagnet $Ba_2CuGe_2O_7$. Much remains to be learned in the study of magnetic critical behavior, as well as the dynamical properties of the soliton lattice, realized in finite fields applied along the *c* axis.

ACKNOWLEDGMENTS

This study was supported in part by NEDO (New Energy and Industrial Technology Development Organization) International Joint Research Grant and the U.S. -Japan Cooperative Program on Neutron Scattering. We thank Scott Moore and Brent Taylor for expert technical assistance. Oak Ridge National Laboratory is managed for the U.S. DOE by Lockheed Martin Energy Research Corporation under Contract No. DE-AC05-96OR22464. Work at Brookhaven National Laboratory was carried out under Contract No. DE-AC02-76CH00016, Division of Material Science, U.S. DOE.

[1] A. Yoshimori, J. Phys. Soc. Jpn. **14**, 807 (1959).
[2] I. Dzyaloshinskii, Sov. Phys. JETP **5**, 1259 (1957).
[3] T. Moriya, Phys. Rev. **120**, 91 (1960).
[4] Y. Ishikawa, K. Tajima, D. Bloch, and M. Roth, Solid State Commun. **19**, 525 (1976).
[5] Y. Ishikawa, T. Komatsubara, and D. Bloch, Physica B **86-88**, 401 (1977).
[6] Y. Ishikawa, G. Shirane, J. Tarvin, and M. Kohgi, Phys. Rev. B **16**, 4956 (1977).
[7] Y. Ishikawa and M. Arai, J. Phys. Soc. Jpn. **53**, 2726 (1984).
[8] C. Wilkinson, F. Sinclair, and J. B. Forsyth (unpublished).
[9] B. Lebech, J. Bernhard, and T. Flertoft, J. Phys.: Condens. Matter **1**, 6105 (1989).
[10] A. Zheludev *et al.*, Phys. Rev. B **54**, 15 163 (1996); see also **55**, 11 879(E) (1997).
[11] A. Zheludev, S. Maslov, G. Shirane, Y. Sasago, N. Koide, and K. Uchinokura, Phys. Rev. Lett. **78**, 4857 (1997).
[12] A. Zheludev, S. Maslov, G. Shirane, Y. Sasago, N. Koide, and K. Uchinokura, Phys. Rev. B (to be published 1 February 1998).
[13] M. Mino *et al.*, Physica B **201**, 213 (1994).
[14] U. Shotte *et al.*, J. Phys.: Condens. Matter **6**, 10 (1994).
[15] T. Ohyama and A. E. Jacobs, Phys. Rev. B **52**, 4389 (1995).
[16] T. Nikuni and A. E. Jacobs, cond-mat/9702201 (unpublished).
[17] L. Heller, M. F. Collins, Y. S. Yang, and B. Collier, Phys. Rev. B **49**, 1104 (1994).
[18] M. Zhitomirsky, O. Petrenko, and L. Prozorova, Phys. Rev. B **52**, 3511 (1995).